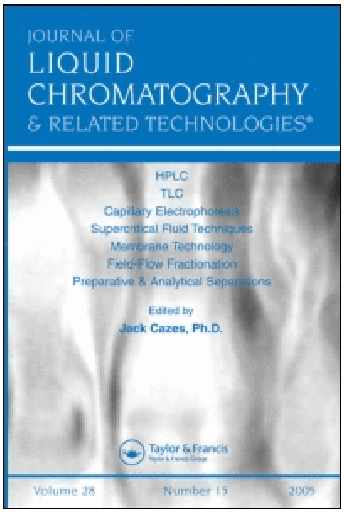

Journal of Liquid Chromatography & Related Technologies
Publication details, including instructions for authors and subscription information:
http://www.informaworld.com/smpp/title~content=t713597273

Data Reduction in Multidetector Size Exclusion Chromatography

Y. Brun[a]
[a] Waters Corporation, Milford, MA

To cite this Article Brun, Y.(1998) 'Data Reduction in Multidetector Size Exclusion Chromatography', Journal of Liquid Chromatography & Related Technologies, 21: 13, 1979 — 2015
To link to this Article: DOI: 10.1080/10826079808006602
URL: http://dx.doi.org/10.1080/10826079808006602

J. LIQ. CHROM. & REL. TECHNOL., 21(13), 1979–2015 (1998)

DATA REDUCTION IN MULTIDETECTOR SIZE EXCLUSION CHROMATOGRAPHY

Y. Brun

Waters Corporation
34 Maple Street
Milford, MA 01757

ABSTRACT

A comprehensive analysis of multidetector size exclusion chromatography (SEC) is presented. The system examined consists of differential refractometer, capillary viscometer, and light-scattering detector combination. New approaches for interpreting multidetector data have been developed. The first one consists in eliminating the concentration chromatogram from the data reduction process. The traces of two molecular-weight-sensitive detectors alone allow calculating molecular weight and intrinsic viscosity distributions of an unknown polymer, assuming the validity of the universal calibration concept for this polymer. This approach can dramatically improve the characterization of polymers with long high-molecular-weight tails, when small amounts of high-molecular-weight fractions are detected by the light-scattering and viscometer detectors, but the concentration is too low to be registered by the refractometer.

Another opportunity discovered is the calculation of the hydrodynamic volume of each fraction of a chromatographed polymer across its distribution, using measured signals from three on-line detectors. This calculation can be performed for any complex polymers, e.g., copolymers or oligomers, even in situations when refractive index increments of molecules depend on retention volume, or columns do not provide full recovery of injected polymer mass. The verification of the universal calibration hypothesis for any unknown polymer is accomplished now by the routine single chromatographic run. The method developed helps to analyze different reasons responsible for the deviation from universal calibration, such as polymer-polymer interactions in solution, band-broadening phenomena, non-steric interactions with a stationary phase or the structural or chemical heterogeneity of a solute. Using triple detection with multiangle light-scattering detector allows, also, to calculate the Flory's viscosity factor across the distribution for polymers with different configurational and conformational structure. The experimental data supporting the theoretical predictions are presented.

INTRODUCTION

Significant expansion of polymer characterization capabilities of SEC centers around on-line molecular-weight-sensitive detectors coupled to a concentration detector[1]. Two most popular combinations are differential refractometer (DR) with continuous capillary viscometer (CV) or DR with light-scattering detector (LS).[2] Each of these dual-detector combinations provides a polymer chemist with important, but partial, information without resort to any column calibration: DR-CV on-line measurements give the intrinsic viscosity distribution,[3,4] DR-LS pair furnishes the molecular weight distribution (MWD) of a polymer.[5]

Only with the universal calibration concept one can complete polymer characterization with a single on-line molecular weight-sensitive detector coupled to a concentration detector. Thus, using hydrodynamic volume-retention volume dependence obtained for a specific chromatographic system from a set of known standards, one can calculate molecular weight of each eluting fraction from the DR-CV measured intrinsic viscosity. The reciprocal relationship permits the deduction of intrinsic viscosity for each monodisperse polymer fraction from the hydrodynamic volume and molecular weight of this fraction obtained from the DR-LS detector combination.[6,7] In addition, the Mark-Houwink coefficients can be determined from a plot of intrinsic viscosity versus molecular weight across the entire molecular weight distribution. The deviation of this plot from the straight line in log-log scale gives the quantitative information about long-chain branching frequency in branched polymers.[8]

Recently, the triple detection SEC with two on-line molecular weight-sensitive detectors (CV and LS) coupled to the concentration (DR) detector was profitably applied to characterization of synthetic[9-18] and biological[19-25] polymers. Obviously, this multidetector (DR-CV-LS) approach eliminates the necessity to use the universal calibration for quantitating an unknown polymer. According to C. Jackson et al.,[26] this circumstance greatly improves the precision and dynamic range of SEC for polymer conformation studies due to insensitivity of results (e.g., the measured Mark-Houwink exponent) to the typical adverse variations in experimental conditions, such as flow rate inconsistency, band-broadening, column deterioration, moderate sample overloading, etc.

In this study, we present further analysis of the triple detector SEC that demonstrates new potentials for polymer characterization. In particular, we show that signals from all three detectors allow the calculation of the hydrodynamic volume through the entire polymer distribution, which provides important information about the polymer structure and the separation mechanism. Another opportunity which has been discovered is the possibility to eliminate the concentration chromatogram from the data reduction process. This approach can dramatically improve the characterization of polymers with small portion of high-molecular-weight material.

EXPERIMENTAL

The SEC was performed with an experimental triple detection system (Waters Corporation, Milford, Massachusetts) consisting of an isocratic model 515 pump, a model 717plus automatic injection module, and three coupled on-line detectors: a model miniDAWN (Wyatt Technology Corp., Santa Barbara, California) three-angle light-scattering detector with a 685 ± 10 nm, 20-mW visible laser diode, differential refractometer, and continuous differential viscometer. The detectors were arranged in series (LS–DR–CV) after the SEC columns. The analog signals from all detectors were collected with sampling rate 10 pps and converted to digital without any filtering. The detector signals were corrected for the corresponding interdetector volumes, calculated from the physical dimensions of the tubings and detector cells.

Two sets of Waters' Styragel (7.8 mm I.D × 300 mm) columns were used for the separation. The first one (set #1) consisted of three 5-μm Styragel columns (two HR 5E mixed bed with effective MW range $2\times10^3 - 4\times10^6$ g/mol, and one HR 3 with effective MW range $5\times10^2 - 3\times10^4$ g/mol). The second set

(set #2) consisted of three 20-μm Styragel columns (two HMW 6E mixed bed with effective MW range 5×10^3 – 10^7 g/mol, and one HMW 2 with effective MW range 10^2 - 10^4 g/mol).

The eluent and the solvent for all polymer samples and standards was filtered HPLC grade tetrahydrofuran (THF, J. T. Baker, Inc., Phillipsburg, NJ), stabilized with 0.025% butylated hydroxytoluene. Operating temperature at column, injector, and pump compartments was 40°C, an injection volume – 300 μL, a nominal flow rate –1.00 mL/min.

Poly(ethyl methacrylate), poly(vinyl acetate) and styrene/acrylonitrile statistical copolymer (acrylonitrile content 32 wt%) were purchased from Scientific Polymer Products, Inc., Ontario, NY.

All polymer solutions were prepared at very low concentrations (less than 0.03 wt%) to avoid possible polymer-polymer interaction effects. Concentrations of 12 narrow polystyrene standards (Waters Corporation) between 2,630 and 4,880,000 g/mol molecular weights ranged from 0.3-0.01-wt%, for low-to-high molecular weights, respectively. These standards were used to construct the corresponding universal calibration curves. The experimental points were fitted by cubic polynomials for both column sets.

RESULTS & DISCUSSION

Ideal Size-Exclusion Separation of Linear Homopolymers. General Approach

If DR is used as a concentration detector, the voltage difference in the detector response due to polymer in solution is proportional to the corresponding refractive index change ΔN. Measuring the pressure drop across a capillary tube over that of the pure solvent with the use of CV, leads to the specific viscosity η_{sp} of a polymer solution.

The intensity of the light scattered by a polymer solution at any given angle θ with respect to the forward direction, above that scattered by the pure solvent, is proportional to the excess Rayleigh ratio R_θ. Low-angle laser light-scattering detectors provide the most important for polymer applications excess Rayleigh ratio at zero angle R_0. Multi-angle light scattering (MALS) data needs to be extrapolated to zero angle to get the value of R_0. Coupled to a SEC system, these three detectors provide continuous measurements of the mentioned above polymer solution properties (ΔN, η_{sp}, R_θ) across the whole chromatogram. Our purpose is to show how these measurements can be converted into quantitative characteristics of macromolecules comprising the polymer sample under investigation.

First, let us consider the case when, at any moment during the chromatographic separation, all three detectors contain monodisperse (or almost monodisperse) polymer fractions in optical cells of photometers or in a capillary of a viscometer. This ideal situation (ideal separation) most probably occurs for linear homopolymers, when macromolecules differ only in their molecular weights, and this brings the molecular weight and the size of a macromolecule into "one-to-one correspondence."

If this is the case, concentration C_i, molecular weight M_i and intrinsic viscosity $[\eta]_i$ of each polymer fraction (slice) i, associated with a particular retention (elution) volume V_i, can be determined from the three detector signals using equations:

$$\Delta N_i = \nu_i C_i \tag{1}$$

$$\eta_{sp,i} / C_i = [\eta]_i (1 + k_H C_i [\eta]_I) \tag{2}$$

$$K_{LS} \nu_i^2 C_i M_i / R_{0,i} = 1 + 2A_2 C_i M_i \tag{3}$$

where

$\nu_i = (dn/dc)_i$ = specific refractive index increment of the polymer fraction, i,

k_H = the Huggins coefficient (is about 1/3 for good solvents and 0.5 - 1 for poor solvents;[28, 29] for hard spheres should be close to 1)[30],

A_2 = second virial coefficient of the polymer-solvent system (is proportional to an effective volume excluded to a macromolecule by another macromolecule in solution), and K_{LS} is a constant for the light-scattering system, given by

$$K_{LS} = 4\pi^2 n_0^2 / \lambda_0^4 N_A \tag{4}$$

where

n_0 = refractive index of the solvent,

λ_0 = wavelength of the incident light in a vacuum,

N_A = Avogadro's number.

Relationships (2) and (3) are well-known Huggins and Zimm equations, respectively, for dilute polymer solutions.[2] Second (concentration) terms in the right sides of these equations reflect, effectively, the polymer-polymer interaction in the solution. In the case of SEC, this interaction should be negligible even in the injected solution; otherwise it could affect the size-exclusion separation of the solute. Concentrations that typically elute from columns are significantly lower than the injected concentrations because of dilution through the columns, and these two concentration terms in equations (2) and (3) are, for the most part, negligibly small. Nevertheless, we will consider the possible consequences of polymer-polymer interactions in the corresponding section of this paper.

The general solution of equations (1) - (3) without regard for polymer-polymer interaction terms has the form,

$$C_i = \Delta N_i / \nu_i \qquad (5)$$

$$[\eta]_i = \eta_{sp,i} \nu_i / \Delta N_i \qquad (6)$$

$$M_i = R_{0,i} / \Delta N_i K_{LS} \nu_i \qquad (7)$$

So far, we have not made any restrictions on the possible values of the refractive index increment ν_i for different polymer fractions. If its magnitude is the same for all fractions: $\nu_i = \nu$, and the chromatographic system provides full recovery of a polymer mass injected, one can calculate ν using appropriate summation (integration) over the whole DR chromatogram:

$$\nu = \rho \Sigma_i(\Delta N_i) / m \qquad (8)$$

where ρ is the volume of a single fraction (slice), and m is the total polymer mass injected. Note that the summation in (8) means nothing more than integration $\nu = \int \Delta N(V)dV/m$ over all elution volumes V, where $\Delta N(V)$ refers to the refractive index change as a function of V. Generally, the magnitude of ν depends on the incident wavelength, especially for the shorter wavelengths. Consequently, it is advisable to use light sources for both photometers with the same or close to each other wavelengths.

Equations (5) - (8) can be used for the calculation of molecular weight and intrinsic viscosity distributions as well as Mark-Houwink coefficients K and α for a linear polymer,

$$[\eta] = KM^{\alpha} \qquad (9)$$

and branching index g' for a branched polymer. These equations do not need universal calibration and can provide accurate polymer characterization even if this calibration fails for any reason; however, each slice i still contains a monodisperse polymer fraction.

Dual Detector Combinations With Universal Calibration

The universal calibration concept adds one more relationship among the molecular parameters of each polymer fraction i:

$$H_i = [\eta]_i M_i \tag{10}$$

where the quantity H is proportional to the hydrodynamic volume of a macromolecule and can be obtained for each elution volume V from the set of polymer standards with known molecular weights:

$$H_i = H_{st,i}. \tag{11}$$

Equation (10) can substitute any one of three equations (1), (2), or (3), or, in other words, the universal calibration (11) can replace any one of three detectors. Thus, using equations (1), (2), (10), and (11), we have conventional routine for DR - CV detector combination.[31] An approach developed by P. M. Cotts[6] for DR - LS pair can be obtained by solving equations (1), (3), (10), and (11).

One can also perform characterization of an unknown polymer without DR detector signal, i.e., using two molecular weight sensitive detectors alone with universal calibration. To do this, one should solve, simultaneously, equations (2), (3), (10), and (11). The solution without concentration terms is:

$$C_i = [R_{0,i}\, \eta_{sp,i} / \nu_i^2 K_{LS}\, H_{st,i}]^{1/2} \tag{12}$$

$$[\eta]_i = [\nu_i^2 K_{LS}\, H_{st,i}\, \eta_{sp,i} / R_{0,i}]^{1/2} \tag{13}$$

$$M_i = [R_{0,i}\, H_{st,i} / \nu_i^2 K_{LS}\, \eta_{sp,i}]^{1/2} \tag{14}$$

These equations allow calculating molecular weight and intrinsic viscosity distributions, Mark-Houwink coefficients, and long-chain branching without refractometer traces. The DR is not needed, even for the calculation of ν for an unknown sample or the universal calibration curve log H_{st} versus V, as we shall subsequently see.

One may use the following summation (integration) over two (CV and LS) chromatograms instead of relationship (8) in this case to calculate the refractive index increment of a polymer:

$$\nu = (\rho / m)\, \Sigma_i [R_{0,i}\, \eta_{sp,i} / K_{LS}\, H_{st,i}]^{1/2} \qquad (15)$$

The CV and LS detectors alone allow to calculate, approximately, the universal calibration curve using a set of polymer samples with narrow MWDs (narrow standards). One can use the summation (integration) over the corresponding chromatograms of each individual standard with injected mass m

$$[\eta]_{st} = (\rho / m)\, \Sigma_i \eta_{sp,i}, \quad M_{st} = (\rho / m\, \nu^2 K_{LS})\, \Sigma_i R_{0,i} \qquad (16)$$

to calculate the "whole polymer" intrinsic viscosity $[\eta]_{st}$ and molecular weight M_{st} of this standard and, thus, its hydrodynamic volume $H_{st} = [\eta]_{st} M_{st}$ as a function of peak elution volume V_{st}, i.e., the universal calibration curve.[32] Note that the integration in equations (16) gives the weight average values of intrinsic viscosity and molecular weight for each individual standard. The narrower the MWDs of the standards, the closer these averages are to the corresponding peak values, and the calculated curve – to the exact calibration curve.

This new approach (12) – (15) can be very effective for quantitating polymer samples with long high-molecular-weight tails (Figure 1), when a small amount of high-molecular-weight fractions is detected by the light-scattering and viscometer detectors, but the concentration is too low to be registered by the refractometer.[2] The typical example of the situation when DR is almost useless for detection and quantitation of high-molecular-weight material is aqueous GPC of Krestin, a complex β-linked proteoglycan biological response modifier.[21,22]

The quantitative analysis of aggregation phenomena in biopolymer solutions[33] is one more area where the use of traces of molecular-weight sensitive detectors only, without resort to the concentration chromatogram, can be highly efficient.

It is well known that the viscoelastic properties of concentrated polymer solutions and melts depend on MWD of polymers. Some of these rheological properties are extremely sensitive to variations in the high-molecular-weight tail of MWD. Thus, the analysis of industrial polypropylenes showed that a very small high-molecular weight fraction of the polymer was enormously

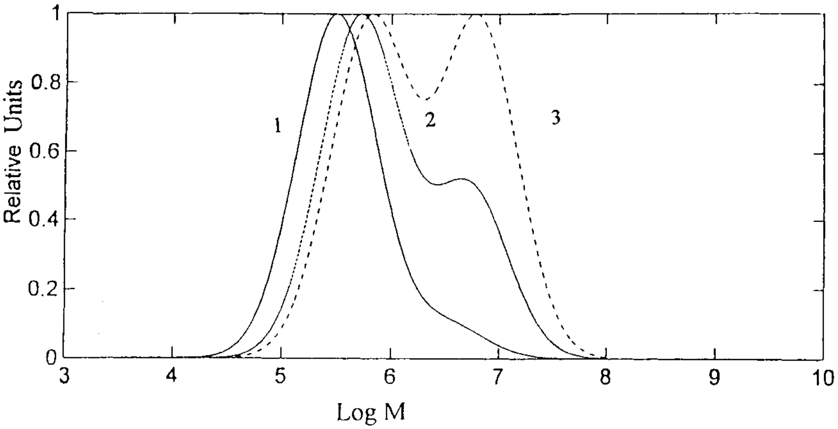

Figure 1. Simulated normalized tracings from DR (1), CV (2) and LS (3) detectors for a hypothetical blend of two samples A and B (in proportion 10 : 1) with Gaussian MWDs (in the logarithmic scale) of the same width (log σ = 0.363), but different peak molecular weights (log M = 5.5 for A and 6.5 for B). Calculated parameters for the blend MWD: M_n = 242,997, M_w = 814,907, M_z = 4,951,930, P = M_w/M_n = 3.35

important for the calculation of dynamic moduli: a total mass fraction of less than a half percent of large molecules is decisive for almost the whole shape of the storage modulus versus frequency curve.[34] The steady-state recoverable compliance J_e^0 is another example of a property that is very sensitive to the tail of the distribution at high molecular weights. The increase of J_e^0 with the broadness of the distribution can reach 2 or 3 orders of magnitude for binary blends whose components are very different in molecular weights.[35] For example, the addition of only 2% of high-molecular-weight polystyrene (2.7×10^6 g/mol) to the polystyrene with molecular weight 10^5 g/mol, increases J_e^0 more than one hundred times.[36] Notice, also, the effects of very low levels of long-chain branching (less than 0.1 branch per 1,000 CH_2) on the rheological behavior in polyethylene.[37]

These branches can reveal themselves in the extremely high-molecular weight edges of the distribution, which probably are not detectable by DR. With this in mind, the following opinion from[34] : " ...gel permeation chromatography (GPC) is hardly a method, which can be used to check the validity of molecular theories on polymer melt rheology" seems reasonable. The approach utilized equations (12)-(15) looks as the real resolution of the issue, because it does not use the concentration chromatogram of the polymer.

Recall that this approach assumes the validity of the universal calibration for the sample under investigation. In the next section, we will show how the triple detection allows calculating the hydrodynamic volume of each slice across the distribution of any polymer and, so, remarkably alleviates the verification of the universal calibration concept.

Hydrodynamic Volume Calculation and Universal Calibration Concept

The hydrodynamic volume for each fraction of an unknown polymer can be calculated from the responses of three detectors independently on the universal calibration obtained from the set of polymer standards. Thus, using definition (10) and equations (1), (2), and (3) without concentration terms, we have:

$$H_i = H_{obs,i} = R_{0,i}\,\eta_{sp,i} / K_{LS}\,\Delta N_i^2 \qquad (17)$$

We call the quantity calculated by this equation as observed hydrodynamic volume H_{obs} to distinguish it from that one calculated from the narrow polymer standards (for which we use, as before, the designation H_{st}). Notice that the right side of equation (17) does not contain the refractive index increments ν_i of different slices. This means that hydrodynamic volume can be calculated for each elution volume for any complex polymer, e.g., copolymer, or oligomers, without any additional measurements or model speculations about the refractive index increment values for eluting macromolecules. Equation (17) does not depend, also, on polymer concentration and can be applied in the situations when the exact mass injected is not known or the columns do not provide full recovery of this mass.

We have performed these calculations (17) for several polymers using chromatograms obtained with Waters' experimental triple detection system (see Experimental section for details). As an example, we demonstrate, here, the results obtained for well-characterized polystyrene sample NBS 706 (Figures 2 - 4).

The values of ΔN_i and $\eta_{sp,i}$ were obtained directly from the DR and CV digitized signals by subtracting corresponding baseline values (Figure 2). The excess Rayleigh ratio $R_{0,i}$ at zero angle for each slice i was calculated in the following way. The light-scattering constant K_{LS} was calculated using values $n_0 = 1.405$ and $\lambda_0 = 685$ nm. The intensities of the light scattered at three angles $\theta = 45°$, $90°$ and $135°$ with respect to the forward direction, were collected with sample rate 10 pps for entire chromatograms. The calibration constant for the light-scattering detector in THF was calculated using the

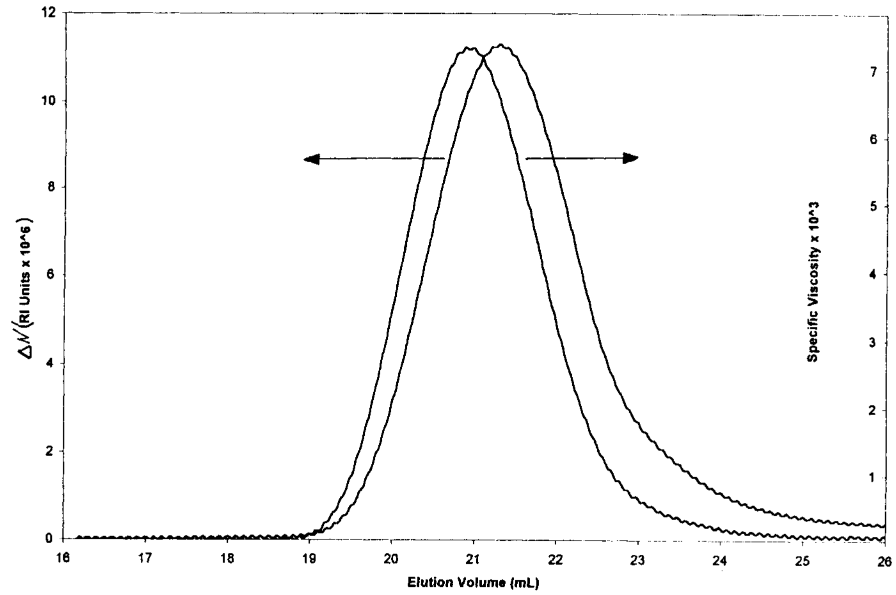

Figure 2. Refractive index change ΔN and specific viscosity η_{sp} measured for the NBS 706 polystyrene sample. Column set #1 (5-μm particle size).

Rayleigh ratio for this solvent ($R_{THF} = 4.4 \times 10^{-6}\,cm^{-1}$). This value was applied to the baseline of the chromatogram obtained at $\theta = 90°$. The intensities of the light at two other angles were normalized using signals from the narrow polystyrene standard with molecular weight 9,000, which should give isotropic light scattering.[5]

The inverse excess Rayleigh ratios R_θ^{-1} for each slice at three angles were extrapolated as a function of $\sin^2(\theta/2)$ to zero angle using linear fit. The intersection with $\theta = 0$ gave R_0^{-1} value according to the formula:

$$R_\theta^{-1} = R_0^{-1} + 16\pi^2 n_0^2 \sin^2(\theta/2)\, r_g / 3\lambda_0^2 R_0 \qquad (18)$$

where r_g is the root mean square (r.m.s.) radius (or radius of gyration) of macromolecules.[2,5] All four curves R_θ versus elution volume V for the NBS 706 sample are shown in Figure 3. Finally, the hydrodynamic volume as a function of elution volume V was calculated using equation (17) (Figure 4).

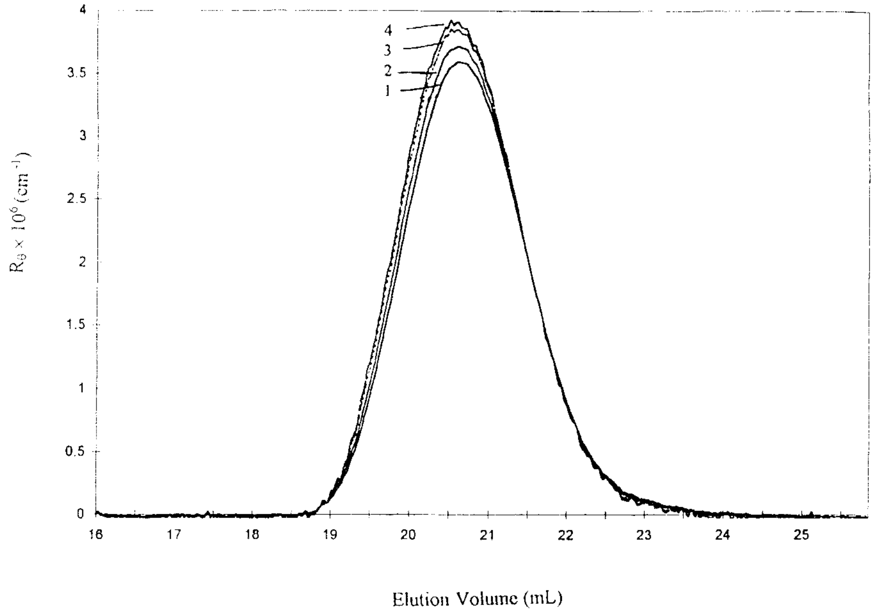

Figure 3. Excess Rayleigh ratios R_0 measured for the NBS 706 polystyrene at θ = 135 (1), 90 (2), 45 (3). R_θ (4) is obtained by linear extrapolation of R_θ as a function of $\sin^2(\theta/2)$. The column set is the same as in Figure 2.

Note that, from this point on, we use deciliters per mole as appropriate units for the hydrodynamic volume defined by equation (10). This corresponds to commonly accepted units for intrinsic viscosity (deciliters per gram) and molecular weight of a polymer (grams per mole). This feature of the triple detection not only opens great opportunities for more complete and accurate characterization of any specific polymer, but can also help to elucidate the separation principle of SEC in general. Thus, the universal calibration concept is of considerable importance in defining the mechanism of SEC. It concerns the equilibrium distribution of macromolecules in confined spaces of complex geometry of porous materials, and is used as a basis for characterization of unknown porous solids via inverse SEC.[38] The verification of this concept, for any complex polymer, can be achieved by the routine single chromatographic run using the foregoing procedure. The universal calibration hypothesis (11) for the polymer under investigation means that

$$H_{obs,i} = H_{st,i} \qquad (19)$$

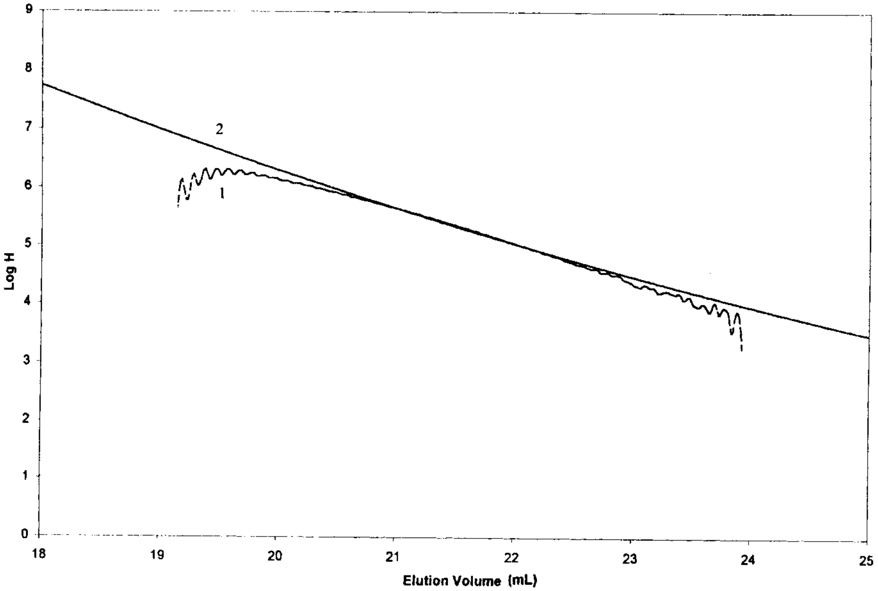

Figure 4. Universal caliberation hypothesis verification for the NBS 706 polystyrene; (1) logarithm of observed hydrodynamic volume calculated from the data depicted in Figures 2 and 3 (Eq. 17), (2) universal calibration curve for the column set #1, third order polynomial fit.

for each polymer fraction i. Figure 4 represents this verification for the NBS 706 sample. The "standard" universal calibration curve (log H_{st} as function of V) for high resolution columns (set #1) was obtained from DR and CV detector chromatograms using 12 narrow polystyrene standards (peak molecular weights from 2,630 to 4,880,000 g/mol). The resulting logarithm of peak hydrodynamic volume H_{st} versus peak retention volume V_{st} was fitted by a cubic polynomial.

Glockner has suggested to call the mode when universal calibration concept asserts as an ideal size-exclusion mechanism.[39] We see that this ideal mode is described by equations (17) and (19). We have used this approach to verify the universal calibration concept for several coil-like polymers, such as poly(ethyl methacrylate), poly(vinyl acetate), and some statistical and block copolymers. One such example (styrene/acrylonitrile copolymer) is depicted in Figure 5. Note that this comparison is made without any adjustable parameters. Small deviations of H_{obs} from H_{st} at the edges of distributions are probably connected with the problem of different sensitivities of the detectors at low- and high-molecular-weight tails.

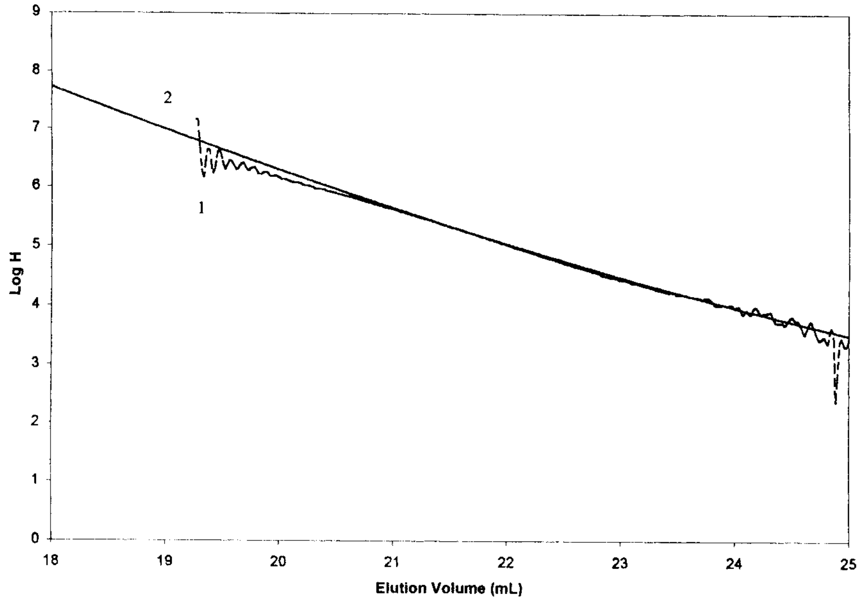

Figure 5. Universal calibration hypothesis verification for styrene/acrylonitrile statistical copolymer with 32% acrylonitrile: (1) logarithm of observed hydrodynamic volume, (2) universal calibration curve for the column set #1.

It is of interest to apply this method, also, to the polymers with different molecular conformations, such as rod- or ball-like, with non-Gaussian distribution of molecular segment density.[30,40] One class of polymers with unusual architecture, highly branched dendritic macromolecules,[12,41] is of special interest.

Viscosity Factor Calculation

The triple detection with multiangle light scattering opens one further opportunity for polymer scientists to attack the problem of universality of large length scale polymer properties in the context of interplay of thermodynamics and dynamics of dilute polymer solutions. Thus, the variation of excess Rayleigh ratio, $R_{\theta,i}$ with angle θ yields r.m.s. radius $r_{g,i}$ at the corresponding slice i according to equation (18). Figure 6 represents the results of this calculation for the NBS 706 polystyrene sample. R.m.s. radius represents the "thermodynamic" size of a macromolecule, whereas the hydrodynamic volume (which is proportional to the volume of equivalent hydrodynamic sphere of

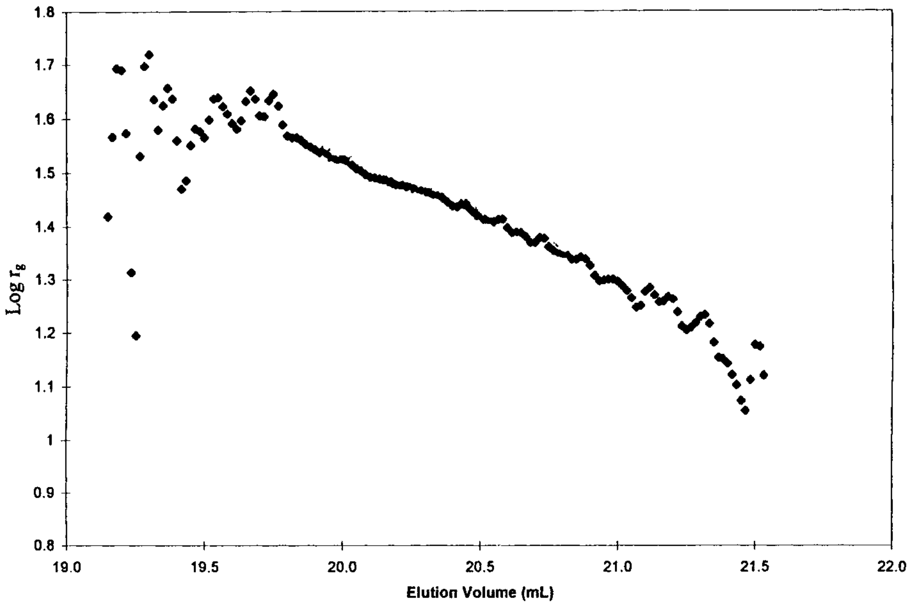

Figure 6. Logarithm of r.m.s. radius (in nanometers) versus elution volume (Eq. 18) for the NBS 706 polystyrene calculated from the experimental data depicted in Figure 3.

radius r_h) – its "hydrodynamic" counterpart, reflecting the hydrodynamic interactions in dilute polymer solutions. The relationship between these two sizes depends on molecular weight, architecture, and shape of macromolecules in dilute solution.

Calculating $H_{obs,i}$ from equation (17), and $r_{g,i}$ from equation (18) we can find the intrinsic viscosity factor (or Flory's viscosity factor) Φ_i,[42] for each individual slice i across the distribution:

$$\Phi_i = H_{obs,i} / (6\, r_{g,i}^2)^{3/2} \tag{20}$$

This factor can be represented, also, as a ratio of the corresponding radii $\phi = r_h/r_g$, where the radius of equivalent hydrodynamic sphere in nanometers $r_h = 0.251\times H^{1/3}$ according to the Einstein viscosity relationship,[42] so that $\phi = 0.615\times \Phi^{1/3}$. Note, again, that the right side of equation (20) contains only the quantities measured directly from three detectors, and does not contain the polymer concentration or refractive index increments v_i of different slices.

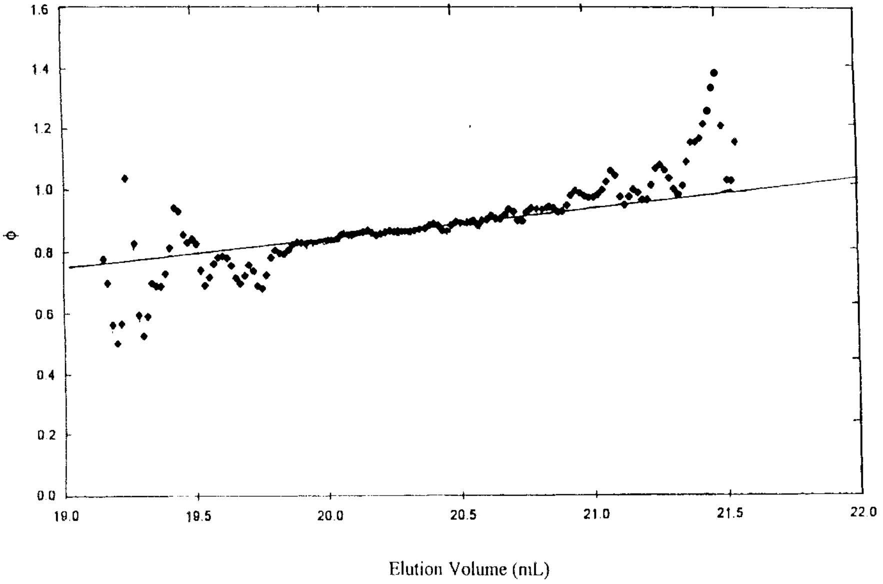

Figure 7. Ratio ϕ of the radius of equivalent hydrodynamic sphere to the r.m.s. radius versus elution volume for the NBS 706 polystyrene calculated from the experimental data depicted in Figures 4 and 6. Straight line is a linear fit to the experimental data

Figure 7 represents ϕ values for the NBS 706 polystyrene sample, calculated with equation (20) from the data depicted in Figures 4 and 6 for $H_{obs,i}$ and $r_{g,i}$, respectively. To our knowledge, the molecular weight dependence of the intrinsic viscosity factor is measured directly for the first time.

The viscosity factor Φ (or ϕ) is one of so-called universal ratios that play a fundamental role in the theory of macromolecules,[42, 43] and the direct and simple experimental method for measuring these quantities can give great insight into the properties of dilute polymer solutions. Flory and Fox[42] calculated Φ for the theta-solution of flexible polymer chains using the Kirkwood-Riseman model of polymer dynamics with the "pre-averaging approximation" of the Oseen tensor[44] representing the hydrodynamic interaction between chain units. They also used "nondraining" limit,[42] which suggested that the fluid within the polymer coil tends to stay entrapped in the coil and not to exchange with the fluid exterior to the coil. The immediate conclusion from this so-called semipermeable coil model is considering the viscosity of polymer solution as the viscosity of a suspension of hard spheres of radii equal to the radius of gyration (the equivalent sphere model).[42] The

Flory-Fox theory leads to the value Φ_{theta} = 3.62 for the unperturbed (theta) condition, if r_g is in nanometers and $[\eta]$ is in deciliters per gram. More recent theoretical approaches without pre-averaging the Oseen tensor give different values for Φ_{theta} (see[29] for review).

For example, Zimm's Monte-Carlo calculations give Φ_{theta} = 2.51,[45] the Gell-Mann-Low type renormalization group method yields the value Φ_{theta} = 2.36.[46] The typical experimental values of Φ_{theta} for polystyrene in cyclohexane at 34.5 – 35 °C (theta-solution) published by different investigators,[48] vary from 1.5 to 2.9.

The renormalization group theory predicts also some decrease of Φ with excluded volume effects in nondraining approximation. Thus, for the "good solvent" limit $\Phi_{good} = 0.707\ \Phi_{theta}$.[43] This gives Φ_{good} = 1.67 or ϕ_{good} = 0.73, which is close to the values obtained for the high molecular weight fractions of NBS 706 sample in THF (Figure 7).

The molecular weight dependence of the viscosity factor depicted in Figure 7 may be related directly to the fact that the quality of a polymer solution improves with the molecular weight of macromolecules. This observation can also explain the wide scatter of the published experimental data for the viscosity factor in good solvents.[46]

Recall that all foregoing theoretical values for the universal ratio Φ are correspond to the infinite molecular weight limit approximation ("when the chain is sufficiently long"[46]) and the nondraining approximation, which is questionable for the case of some polymers in good solvents, particularly for the polystyrene.[47]

Note that only the nondraining limit leads to the constant values of Φ asymptotically independent of the molecular weight of the flexible polymer chain.

Some "draining" effects could take place in the case of moderate molecular weight polystyrene in THF, with more degree for lower molecular weight fractions. For stiff coils, where the nondraining approximation breaks down completely, we may expect more significant deviation from the horizontal line of the calculated from formula (20) elution volume dependence of Φ.

The approach developed can also help to verify independently the exponents found for the viscosity law (Mark-Houwink) and conformation plots for polymers with different macromolecular architecture.[12,30]

Hydrodynamic Volume Calculation and System Parameters

The foregoing hydrodynamic volume calculation can help in establishing the correct values of multidetector system parameters, such as instrument calibration constants or interdetector volume, which provide accurate polymer characterization. In such a manner, this calculation can serve as an additional tool for a systematic approach developed[49] for diagnosing and overcoming problems in multidetector SEC analysis, providing the universal calibration concept (19) asserts.

Let us consider just one example. If the light sources for DR and LS photometers have different wavelengths, the corresponding refractive index increments ν_{DR} and ν_{LS} for the same polymer-solvent system may differ also, because ν depends on wavelength.[50] Consequently, equations (1) – (3) (without concentration terms) become:

$$\Delta N_i = \nu_{DR,i}\, C_i \tag{21}$$

$$\eta_{sp,i} / C_i = [\eta]_i \tag{22}$$

$$K_{LS}\nu_{LS,i}^2 C_i\, M_i / R_{0,i} = 1 \tag{23}$$

Using definition (11) and universal calibration hypothesis (19) we obtain from equations (21) – (23) for each slice i of a polymer distribution

$$\nu_{LS,i} \;/\; \nu_{DR,i} = (R_{0,i}\,\eta_{sp,i} \,/\, K_{LS}\, H_{st,i}\,\Delta N_i^2)^{1/2} \tag{24}$$

Usually, it is not an easy matter to find published ν values for different wavelengths. Equation (24) allows calculating refractive index increments of each fraction of a polymer for one photometer, if the corresponding values for another with different wavelength are known and the universal calibration curve log H_{st} versus V is established. This allows also estimating the effect of difference in wavelengths on the observed MWDs.

Non-Ideal Size-Exclusion Separation

There are several factors, which can cause the disruption of the ideality of size-exclusion separation described by equation (19), even for the Gaussian homopolymer chains, when formula (17) does not provide the correct values of the hydrodynamic volume of macromolecules. These are interaction between polymer chains in solution, their non-steric interaction with a stationary phase, and instrumental band broadening phenomena. We continue to call the quantity calculated from equation (17) as observed hydrodynamic volume, even in the situation when these effects take place.

Now, let us demonstrate how the triple detection can give an elucidating glimpse into the polymer characterization for these three cases, each of which we consider separately. Note that we do not consider, here, the case of low-molecular-weight polymers and oligomers (molecular weight of the order or less than 10^3 g/mol).

The failure of the universal calibration concept for these products, among other things, can be caused by lacking the general configuration statistics inherent in polymer chains.

Polymer - Polymer Interaction

If the concentration of a polymer solution inside detectors' cells is not low enough for the concentration terms in equations (2) and (3) to be ignored, we have a situation when a polymer-polymer interaction may have an impact on both separation and detection.

The general solution of equations (1) - (3) has the form,

$$C_i = \Delta N_i / v_i \tag{25}$$

$$[\eta]_i = \frac{\eta_{sp,i} v_i}{\Delta N_i (1 + Q_{\eta,i})} \tag{26}$$

$$M_i = \frac{R_{0,i}}{\Delta N_i K_{LS} v_i (1 + Q_{\eta,i})(1 - Q_{R,i})} \tag{27}$$

where terms

$$Q_{\eta,i} = \left(\sqrt{1 + 4\eta_{sp,i} k_H} - 1\right)/2, \quad Q_{R,i} = \frac{2A_2 R_{0,i}}{K_{LS} v_i^2}$$

are responsible for the polymer-polymer interaction in the solution.

Using the definitions (10) and (11), equations (26) and (27), we have, for the hydrodynamic volume, in this case:

$$H_{obs,i} = R_{0,i}\,\eta_{sp,i} / K_{LS}\,\Delta N_i^2\ (1 + Q_{\eta,i})^2 (1 - Q_{R,i}) \tag{28}$$

The measured hydrodynamic volume (17) now depends on refractive index increments ν_i of each slice i, and other parameters specific for a given polymer, such as the second virial coefficient A_2 and Huggins constant k_H. It makes the universal calibration hypothesis (19) questionable, when polymer-polymer interaction should be taken into account, and the triple detection with equations (25) - (27) remains the only approach for accurate and complete polymer characterization.

If analysts still want to use universal calibration as an approximation in this case, they also may use the dual detection methods for polymer characterization. However, the concentration terms in corresponding equations should be taken into account. Thus, for the polymer characterization without a concentration detector (with two molecular-weight-sensitive detectors only and universal calibration), the following equations should be used,

$$C_i = [R_{0,i}\,\eta_{sp,i} / \nu_i^2 K_{LS}\,H_{st,i} (1 + Q_{\eta,i}) (1 - Q_{R,i})]^{1/2} \tag{29}$$

$$[\eta]_i = [\nu_i^2 K_{LS}\,H_{st,i}\,\eta_{sp,i} (1 - Q_{R,i}) / (1 + Q_{\eta,i})\,R_{0,i}]^{1/2} \tag{30}$$

$$M_i = [R_{0,i}\,H_{st,i} (1 + Q_{\eta,i}) / \nu_i^2 K_{LS}\,\eta_{sp,i} (1 - Q_{R,i})]^{1/2} \tag{31}$$

instead of more simple equations (12) - (14).

Non-Steric Interactions

Another reason for the deviation from the ideal size-exclusion separation is non-steric interaction between a solute and a stationary phase during the separation.[31] The consequence of this interaction could be the shift of the retention volume to the lower or (more likely) higher values as against the size-exclusion effects only.

This interaction can be caused by repulsive forces (e.g., electrostatic repulsion in aqueous eluents with high values of dielectric constant), as well as by attractive forces (which can have the same origin as for adsorption chromatography, reversed phase chromatography, ion-exchange chromatography, etc.). These extra effects normally do not cause the appearance of any local polydispersity (i.e., polydispersity of individual slices after separation). Because of this, the triple detection allows to quantitate the unknown polymer using equations (12) - (14) (or (25) - (27)) in this case.

However, the observed hydrodynamic volume $H_{obs}(V)$, as function of elution volume V calculated from equation (17), shifts from the position $H_{st}(V)$, predicted from the universal calibration curve, towards higher or lower values: $H_{obs}(V) < H_{st}(V)$ for repulsive and $H_{obs}(V) > H_{st}(V)$ for attractive forces. Thus, the calculation of $H_{obs}(V)$ using the triple detection provides a means for the estimation of non-steric effects of separation. Let us analyze this feasibility of the triple detection in some detail.

In the general case, the observed distribution coefficient K_{obs} of a polymer solute can be subdivided into two parts,

$$K_{obs} = K_{SEC} K_{int} \tag{32}$$

where K_{SEC} describes the ideal entropy-driven distribution of solute molecules between interstitial and pore volume (ideal size-exclusion mechanism[39]) and K_{int} is the additional contribution from the non-steric interactions. The quantity K_{SEC} can be described with reference to the conformational entropy loss $\Delta S < 0$ due to restriction of macromolecule fluctuation motion inside pores: $K_{SEC} = \exp(\Delta S/R)$ (R is the universal gas constant). Analogously, K_{int} is associated with the energy ΔE of interaction with the stationary phase: $K_{int} = \exp(-\Delta E/RT)$ (T is absolute temperature), so that $\Delta E > 0$ for repulsive forces and $\Delta E < 0$ for attractive interactions. In such a manner, the distribution constant K_{obs} is described by the free energy change $\Delta G = \Delta E - T\Delta S$ due to both size-exclusion and non-steric interactions: $K_{obs} = \exp(-\Delta G/RT)$. If steric effects still predominate so that $-T\Delta S > -\Delta E$, then $-\Delta G$ is negative, K_{obs} is less than 1, and we still have the size-exclusion mode of separation, when retention time decreases as molecular weight of polymer homologues increases.

Note that, for high molecular weight molecules, both ΔS and ΔE are usually proportional to M:

$$\Delta S = M\,\Delta s, \quad \Delta E = M\,\Delta e \tag{33}$$

where Δs and Δe are corresponding specific values, which do not (or almost do not) depend on M.[51] This means that, although the effect of non-steric interactions becomes more pronounced with the increase of molecular weight of polymer homologues, the size-exclusion mode takes place for all polymer homologues simultaneously as long as $-T\Delta s > -\Delta e$.

By definition, the distribution constant is related to the observed elution volume V by the retention equation[52]

$$V = V_I + K_{obs} V_P \tag{34}$$

where V_I and V_P are correspondingly the interstitial (exclusion) and pore volumes of columns. Analogously, elution volume V_{SEC} for the ideal size-exclusion mode is given by equation

$$V_{SEC} = V_I + K_{SEC} V_P \tag{35}$$

Combining equations (32), (34), and (35), we have, finally:

$$K_{int} = (V - V_I) / (V_{SEC} - V_I) \tag{36}$$

In such a manner, measuring V and V_{SEC}, for each polymer fraction eluted, allows for the estimation of the adsorption or any other non-steric interaction between solute macromolecules and a stationary phase, through the calculation of energy of the corresponding interaction $\Delta E = - RT \ln K_{int}$ as a function of V.

Let us show how to perform this measurement using triple detection and universal calibration. The observed hydrodynamic volume H_{obs} for each elution volume V can be calculated from the signals of three detectors using formula (17), which we rewrite using elution volume V instead of index i to indicate the point at the chromatogram (so that H_{obs} (V) refers to the hydrodynamic volume as a function of V while $H_{obs,i}$ indicates a particular value of H_{obs} at a particular volume, V_i):

$$H_{obs}(V) = R_0(V)\ \eta_{sp}(V) / K_{LS} \Delta N^2(V) \tag{37}$$

The universal calibration curve obtained from narrow standards, without any non-steric interactions, provides the value of elution volume V_{SEC} corresponding to H_{obs} for the ideal mode (see dashed horizontal line in Figure 8):

$$H_{obs}(V) = H_{st}(V_{SEC}) \tag{38}$$

For example, suppose the universal calibration is given by equation

$$H_{st}(V) = H_0 \exp(-V/V_H), \tag{39}$$

where the parameter V_H determines the slope of the curve and can depend on the elution volume V in the case of non-linear calibration. Then

$$V_{SEC} = V_H \ln[H_0 / H_{obs}(V)] = V_H \ln [H_0 K_{LS} \Delta N^2(V) / R_0 (V) \eta_{sp}(V)] \qquad (40)$$

Substituting expression (40) for V_{SEC} into formula (36) gives the quantity of K_{int} (or ΔE) for each eluting polymer fraction. Note, again, that this calculation does not depend on refraction index increment of macromolecules and can be performed for any complex polymer or oligomer.

The weak non-steric effects roughly give a rotation of observed hydrodynamic volume around the point corresponding to the total $V_{total} = V_I + V_P$ volume of the system (Figure 8).

The positive rotation (clockwise) corresponds to attractive forces, and the negative (counter-clockwise) to repulsive forces. This qualitative conclusion depicted at Figure 8 results from the equations (36) and (40) which can be put in the form:

$$\ln [H_{obs}(V)/H_{st}(V)] = (V - V_I)(K_{int} - 1) / K_{int} V_H \qquad (41)$$

For adsorption effects, $K_{int} > 1$ and $H_{obs}(V) > H_{st}(V)$ for all V, for repulsive forces, $K_{int} < 1$ and $H_{obs}(V) < H_{st}(V)$. For relatively low-molecular-weight fractions eluted not too far from V_{total},, $| K_{int} - 1 | \approx | M \Delta e / RT | << 1$ and the ratio $H_{obs}(V)/H_{st}(V) \approx 1 - M \Delta e V_P / RT V_H$ is very close to 1. The deviation of this ratio from 1 increases with increasing molecular weight M (or decreasing retention volume V).

Closer to the exclusion volume V_I, the values of K_{int} can become significantly greater or less than 1 in the cases of adsorption or repulsive interactions respectively, and we have from (41):

$$\ln [H_{obs}(V)/H_{st}(V)] = (V - V_I) / V_H, \quad (\Delta e < 0, K_{int} >> 1), \qquad (42)$$

$$\ln [H_{obs}(V)/H_{st}(V)] = -(V - V_I) / K_{int} V_H, \quad (\Delta e > 0, K_{int} << 1) \qquad (43)$$

From equation (42), we can see that the difference between values of $H_{obs}(V)$ and $H_{st}(V)$ asymptotically does not depend on the energy of attractive interaction for high-molecular-weight fractions of a polymer. The opposite situation takes place for repulsive forces (equation (43)): the non-steric interaction has a dominant role in measured hydrodynamic volume behavior through all elution volumes including the region close to V_I.

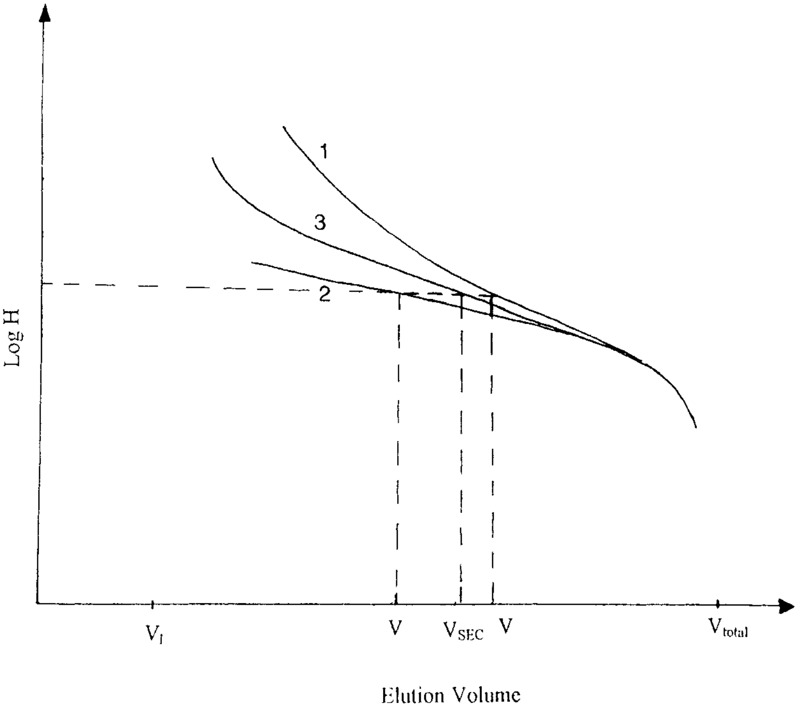

Figure 8. A schematic sketch of observed hydrodynamic volume in the cases of attractive (1) or repulsive (2) non-steric interactions between a solute and a stationary phase, (3) universal calibration curve.

Instrumental Band Broadening

Let us consider one more factor which can cause the deviation from the ideal size-exclusion mechanism: band broadening phenomena.[31] These phenomena lead to the local polydispersity of a polymer even after size-exclusion separation: each slice contains macromolecules with different size, and, therefore, different molecular weights, intrinsic viscosities, and hydrodynamic volumes. As a result of this, instead of instant values of molecular weight and intrinsic viscosity given by equations (6) and (7), on-line detectors measure weight average values for the local distribution of each fraction i:

$$[\eta]_{w,i} = \eta_{sp,i} v_i / \Delta N_i, \qquad (44)$$

$$M_{w,i} = R_{0,i} / K_{LS} \nu_i \Delta N_i \quad (45)$$

Using, again, elution volume V instead of index i, we should replace equations (5) - (7) with the following:

$$C(V) = \Delta N(V) / \nu(V), \quad (46)$$

$$[\eta]_w(V) = \eta_{sp}(V)\nu(V) / \Delta N(V), \quad (47)$$

$$M_w (V)= R_0(V)/ K_{LS} \nu(V) \Delta N(V) \quad (48)$$

Here C(V) stands for the concentration detector response at elution volume V and should be deconvolved using Tung's equation to get corrected for band broadening "standard" value C_{st} (V).[31,53]

Band broadening is determined by the shape of the spreading function. As an example, consider the axial dispersion in the case of the symmetrical Gaussian type instrumental band-broadening function with the variance σ, which can be determined from the set of narrow standards.[31] The more general case of the skewed peak model of the exponentially modified Gaussian function[31,54] can be considered in a similar way, and qualitatively leads to the same results that follow.

The key problem here is the calculation of σ and the corrected for axial dispersion (or "standard") molecular weight and intrinsic viscosity calibration curves of the polymer under investigation:

$$[\eta]_{st}(V) = [\eta]_0 \exp(-V / V_\eta), \quad M_{st}(V) = M_0 \exp(-V / V_m) \quad (49)$$

The parameters of these curves, V_η and V_m, determine the slopes of the corresponding calibration curves and can also depend (as well as variance σ) on the elution volume V in the case of non-linear calibration.[53] These parameters are essential for the calculation of corrected molecular weight and intrinsic viscosity distributions, statistical moments of these distributions, as well as Mark-Houwink coefficients[31,55,56] $\alpha = V_m / V_\eta$, $K = [\eta]_0 / M_0^\alpha$. Let us see how different detector combinations, including the triple detection, allow to calculate these parameters.

It is convenient to introduce spreading volumes of the system associated with the intrinsic viscosity and molecular weight calibrations, respectively:

$$V_{\sigma\eta} = \sigma^2 / 2V_\eta, \quad V_{\sigma m}= \sigma^2 / 2V_m \quad (50)$$

The theory of the axial dispersion correction holds only when the instrumental spreading does not disturb calibration curves significantly. This means that $V_{\sigma\eta} \ll V_\eta$, $V_{\sigma m} \ll V_m$.

In the case under consideration, the equations (46) - (48) can be supplemented by the relationships[57,58]

$$[\eta]_{st}(V) = \exp(-V_{\sigma\eta}/V_\eta)\,[\eta]_w(V)\,C(V)\,/\,C(V - 2V_{\sigma\eta}) \qquad (51)$$

$$M_{st}(V) = \exp(-V_{\sigma m}/V_m)\,M_w(V)\,C(V)\,/\,C(V - 2V_{\sigma m}) \qquad (52)$$

Substituting from equations (46) - (50) into equations (51), (52), and rearranging, gives:

$$[\eta]_0 \exp(-V/V_\eta) = \eta_{sp}(V + V_{\sigma\eta})\,v(V - V_{\sigma\eta})\,/\,\Delta N(V - V_{\sigma\eta}), \qquad (53)$$

$$M_0 \exp(-V/V_m) = R_0(V+V_{\sigma m})\,v(V-V_{\sigma m})\,/\,K_{LS}\,\Delta N(V-V_{\sigma m})\,v^2(V+V_{\sigma m}) \qquad (54)$$

Equation (53) provides the calculation of parameters of the corrected intrinsic viscosity calibration curve using the DR and CV signals, even for nonlinear case (V_η depends on V), if the spreading function variation $\sigma = \sigma(V)$ is known. Applying equation (53), simultaneously, to two or more polymer samples with the same chemical structure (that is, with the same values of parameters V_η, $V_{\sigma\eta}$ and $[\eta]_0$) allows to calculate the values of σ.

It is possible, also, to obtain the corrected molecular weight calibration curve from this equation (53) if the universal calibration curve from the narrow standards is added to the DR - CV detector combination,[56]

$$H_{st}(V) = H_0 \exp(-V/V_H), \quad H_0 = [\eta]_0 M_0, \quad 1/V_H = 1/V_\eta + 1/V_m \qquad (55)$$

Analogously, equation (54) for the DR - LS detector combination provides the calculation of the corrected molecular weight calibration curve[59] and, when applied to more than one polymer with the identical chemical composition, of the instrumental spreading function.

Combining this equation with the expression for the "standard" hydrodynamic volume (55) gives also the parameters for corrected viscosity calibration curve.

We can exclude the DR response ΔN from equations (53) and (54):

$$\frac{\eta_{sp}(V-2V_{\sigma m})}{[\eta]_0 \exp[(2V_{\sigma m}+V_{\sigma\eta}-V)/V_\eta]} = \frac{R_0(V-2V_{\sigma\eta})}{M_0 K_{LS} \nu^2 (V-2V_{\sigma\eta}) \exp[(2V_{\sigma\eta}+V_{\sigma m}-V)/V_m]} \tag{56}$$

This equation uses two molecular weight sensitive detector responses only and permits the calculation of corrected calibration curves if combined with the universal calibration (55). Analogously, ΔN can be removed from the equation (46) using relationships (53) or (54):

$$C(V) = \frac{\eta_{sp}(V+2V_{\sigma\eta})}{[\eta]_0 \exp[-(V+V_{\sigma\eta})/V_\eta]} \tag{57}$$

Equation (57) allows not to use the DR even for the deconvolution of the concentration chromatogram. Note that the right side of this equation does not depend on the refractive index increment of a polymer.

Only the triple detection combination allows for the use of both equations (53) and (54) simultaneously for the calculation of corrected calibration curves and, thus, of the Mark-Houwink coefficients, without universal calibration. This is the obvious advantage of the triple detection SEC. Nevertheless, it is pertinent to note that equations (53), (54), and (56) strongly depend on refraction index increment of the polymer fractions. This feature may present a problem for copolymers with the refractive index increment depending on elution volume. Because of this, we can recommend another approach to the axial dispersion correction with the triple detection for the case of complex polymers with the compositional drift.

Multiplying equations (53) and (54) and simple rearrangement gives:

$$H_{obs}(V)/H_{st}(V) = \exp[V_{\sigma\eta}/V_\eta + V_{\sigma m}/V_m]\, \Delta N(V-2V_{\sigma\eta})\, \Delta N(V-2V_{\sigma m})/\Delta N^2(V) \tag{58}$$

where $H_{obs}(V)$ is given by formula (37). Deriving equation (58), we have neglected the difference of the ratio $\nu^2(V)$ / $[\nu(V - 2V_{\sigma\eta})\ \nu(V - 2V_{\sigma m})]$ from unity. This is a very good approximation, because the refractive index increments of different fractions can depend on their chemical composition, but not on concentration. Recall, also, that both spreading volumes $V_{\sigma\eta}$ and $V_{\sigma m}$

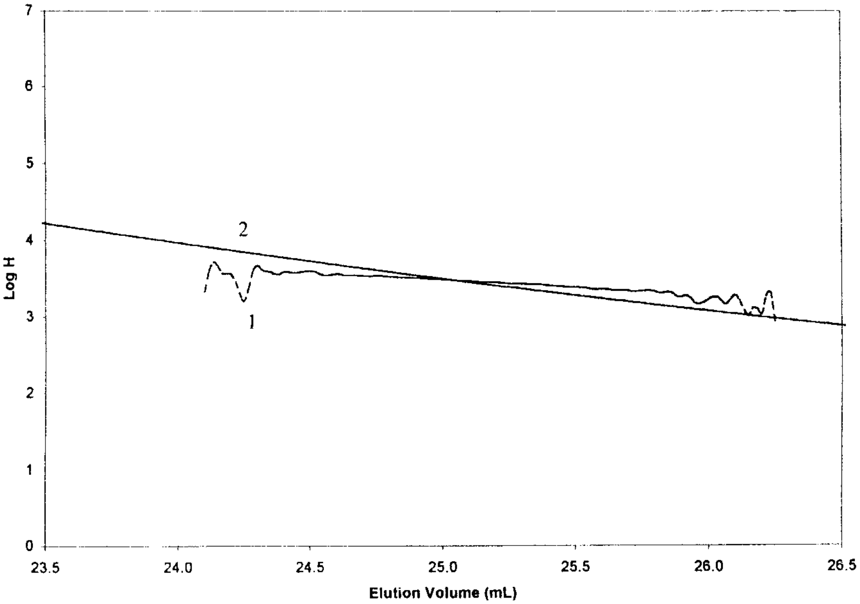

Figure 9. Effect of the axial dispersion on observed hydrodynamic volume (1) for the narrow polystyrene standard (peak molecular weight 18,000 g/mol), (2) universal calibration curve for the column set #1.

are significantly less than V. Adopting equation (58) and the universal calibration curve (55), we can calculate the corrected calibration curves for any complex polymers, including copolymers, without any information about their refractive index increments, because the right side of this equation does not depend (or almost does not depend) on ν. In the same manner, equation (57) can be used for the deconvolution of the concentration profile for copolymers with a compositional drift. Equation (58) may also be applied to two or more samples with the same chemical structure to perform calibration and axial dispersion correction simultaneously. This approach necessitates the triple detection and universal calibration.

One can see, from equation (58), that the axial dispersion rotates the hydrodynamic volume in a counter-clockwise direction about the point corresponding to an apex of the concentration chromatogram: $H_{obs}(V) < H_{st}(V)$ if $V < V_{apex}$ and $H_{obs}(V) > H_{st}(V)$ if $V > V_{apex}$, by the angle depending on the shape of the chromatogram. For more narrow distribution, this rotation is more significant. These qualitative conclusions are supported by

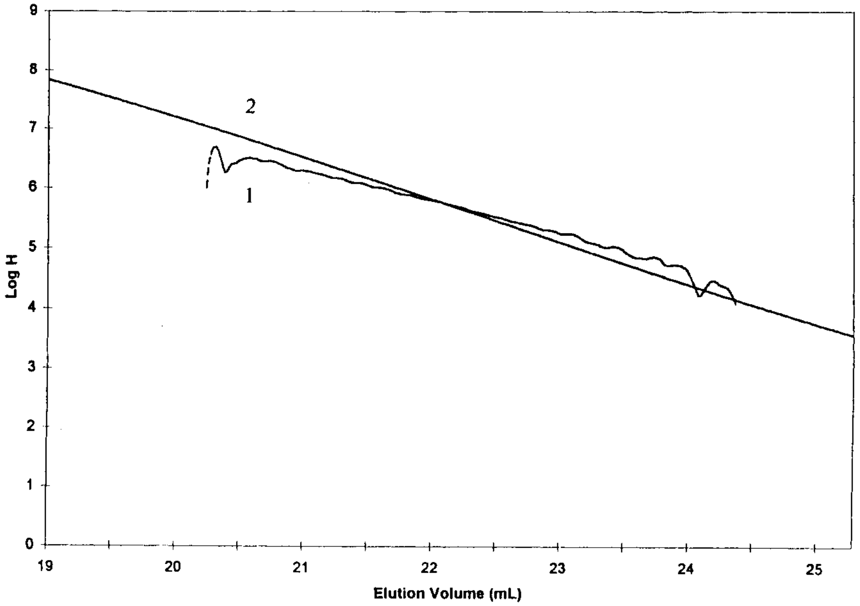

Figure 10. Effect of axial dispersion on observed hydrodynamic volume (1) for the broad polystyrene sample NBS 706, (2) universal calibration curve for the column set #2 (20-μm particle size), third order polynomial fit.

experimental results presented in Figures 9 and 10. All calculations were performed in a similar manner as described above in the section "Hydrodynamic Volume Calculation and Universal Calibration Concept." Figure 9 shows the results for the narrow polystyrene sample with peak molecular weight 18,000 g/mol and polydispersity less than 1.04.

We see that, even for the 5-μm particle size columns, the axial dispersion cannot be neglected completely in the case of narrow MWD samples. Results for larger particle size (20-μm) columns (set #2) are shown at Figure 10. These columns generate more significant axial dispersion, which causes remarkable deviation from the ideal separation.

We see that the observed hydrodynamic volume H_{obs} versus V dependence differs from the peak calibration curve, even for a relatively broad sample. The deviation measured can be used for the axial dispersion correction of the experimental chromatograms.

SEC of Polymer With Complex Molecular Structure

Another contributor of the local polydispersity can be the structural or chemical heterogeneity of a polymer, when macromolecules with different molecular weights may have the same size due to the difference in the chemical composition or molecular structure (e.g., copolymer with compositional drift or polymers with nonuniform long-chain branching).[60-62] As a result of this, each elution volume can be associated with remarkable local molecular weight and intrinsic viscosity distributions of a solute. The fundamental distinction between this case and the instrumental band broadening is the dissimilar local hydrodynamic volume distributions. The instrumental spreading causes the hydrodynamic volume polydispersity in the same manner as for molecular weight and intrinsic viscosity polydispersities. In the case of complex polymers, at any instant macromolecules in the detector cell have the same (or almost the same) hydrodynamic volume, in spite of the differences in their molecular weights and intrinsic viscosities, and this volume should coincide with the corresponding value H_{st} at the universal calibration curve. But equation (17) does not provide this correct value of H in the case of complex polymers, as it does for homopolymers. Let us show what property of macromolecules can be measured using equation (17) in the case of macromolecules with complex microstructure.

As in the case of band broadening, weight average intrinsic viscosity $[\eta]_{w,i}$ and molecular weight $M_{w,i}$ for each slice i can be calculated from equations (44) and (45). It is possible, also, to calculate corresponding number average values for each polymer fraction using a universal calibration curve obtained from the narrow standards:[60,61]

$$M_{n,i} = H_{st,i} / [\eta]_{w,i} = H_{st,i}\, \Delta N_i / \eta_{sp,i}\, \nu_i \tag{59}$$

$$[\eta]_{n,i} = H_{st,i} / M_{w,i} = H_{st,i}\, K_{LS}\, \nu_i\, \Delta N_i / R_{0,i} \tag{60}$$

The polydispersity $P_i = M_{w,i} / M_{n,i} = [\eta]_{w,i} / [\eta]_{n,i}$ of the local polymer distribution may be obtained from the ratio of equations (44) and (60) (or (45) and (59)):

$$P_i = R_{0,i}\, \eta_{sp,i} / K_{LS}\, \Delta N_i^2\, H_{st,i} \tag{61}$$

Note that the right side of equation (61) does not contain the refractive index increment ν_i in the same way as of equation (17). This means that the local polydispersity, as a function of retention volume, can be measured for any complex polymer, including copolymers, using three detectors and the universal calibration curve. No assumption about the refractive index increment values for eluting macromolecules should be made.

Let us continue to call the quantity calculated by equation (17) as observed hydrodynamic volume $H_{obs,i}$, even if the actual hydrodynamic volume of macromolecules in this case is $H_{st,i}$. Since the polydispersity cannot be less than 1, the local heterogeneity caused by the structural or chemical heterogeneity of the polymer always leads to an increase of calculated from equation (17) hydrodynamic volume H_{obs} compared with its real value H_{st}, obtained from the narrow standards:

$$H_{obs,i} = P_i H_{st,i} \tag{62}$$

According to equation (62), in the logarithmic scale, which is usually used for the universal calibration curve presentation, the difference between these two values is determined by the polydispersity P(V) of the local distribution of a complex polymer, caused by its compositional drift or any other structural heterogeneity:

$$\log H_{obs}(V) - \log H_{st}(V) = \log P(V) \tag{63}$$

Equations (5), (44), (45), (59), and (60) allow to calculate weight average and number average molecular weight and intrinsic viscosity distributions of any polymer. But these distributions depend not only on its own (true) molecular weight and intrinsic viscosity polydispersity, but also on the local heterogeneity across the whole chromatogram. The deviation of the observed hydrodynamic volume H_{obs} from the corresponding point at the universal calibration curve H_{st} can serve as a measure of this heterogeneity. To obtain the true molecular weight and/or intrinsic viscosity distributions of the complex polymer, we should make some additional assumptions about its molecular structure (e.g., determine dependence of chemical composition on molecular weight of a macromolecule). In any case, the difference (63) between the observed and real values of the hydrodynamic volumes gives useful information about structural heterogeneity of polymers under investigation.

CONCLUSION

The calculation of the hydrodynamic volume across the polymer distribution, using measured signals from three on-line detectors, allows to gain a better insight into the mechanism of separation and the structures of macromolecules. Verification of universal calibration concept and the viscosity ratio measurements are the most important benefits of applying this method. Different reasons for the deviation from the universal calibration, such as polymer-polymer interactions in solution, band-broadening phenomena, non-steric interactions with a stationary phase, or the structural or chemical heterogeneity of a solute lead to qualitatively different hydrodynamic volume versus elution volume dependencies, and can be clearly discernible in experimental curves.

The calculation of the viscosity factor Φ across the distribution for polymers with different configurational and conformational structure helps to gain a better understanding of large-scale equilibrium and dynamical polymer properties.

Molecular-weight sensitive detectors proved to be very effective for detecting and quantifying small portions of high-molecular-weight material, such as aggregates, highly branched polymer fractions, etc.

The opportunity to eliminate the concentration chromatogram completely from the data reduction process for the polymers of this kind may significantly improve the accuracy and precision of the data.

REFERENCES

1. S. T. Balke, "Characterization of Complex Polymers by Size Exclusion Chromatography and High-Performance Liquid Chromatography," in **Modern Methods of Polymer Characterization**, H. G. Barth, J. W. Mays, eds., John Wiley & Sons, Inc., New York, 1991, pp. 1-66.

2. C. Jackson, H. G. Barth, "Molecular Weight-Sensitive Detectors for Size Exclusion Chromatography," in **Handbook of Size Exclusion Chromatography**, Chi-san Wu, ed., Chromatographic Science Series, v. 69, Marcel Dekker, Inc., New York, 1995, pp. 103-145.

3. W. W. Yau, Chemtracts: Macromol. Chem., **1**, 1-36 (1990).

4. W. W. Yau, S. W. Rementer, J. Liq. Chromatogr., **13**, 627-675 (1990).

5. P. J. Wyatt, Analytica Chimica Acta, **272**, 1-40 (1993).

6. P. M. Cotts, J. Polym. Sci., Polym. Phys. Ed., 24, 1493-1507 (1986).

7. P. J. Wyatt, D. W. Shortt, "Light Scattering Viscometry," in **Proceedings, International GPC Symposium**, San Francisco, CA, 1991, pp. 65-81.

8. A. Rudin, "Measurement of Long-Chain Branch Frequency in Synthetic Polymers," in **Modern Methods of Polymer Characterization**, H. G. Barth, J. W. Mays, eds., John Wiley, Inc., New York, 1991, pp. 103-112.

9. J. Lesec, G. Volet, J. Liq. Chromatogr., **13**, 831-849 (1990).

10. D. J. Nagy, D. A. Terwilliger, "SEC of Poly (Vinyl Alcohol) Using Multi-Detection Methods" in **Proceedings, International GPC Symposium**, San Francisco, CA, 1991, pp. 161-179.

11. S. Pang, A. Rudin, Polymer, **33**, 1949-1952 (1992).

12. T. H. Mourey, S. R. Turner, M. Rubinstein, J. M. J. Frechet, C. J. Hawker, K. L. Wooley, Macromolecules, **25**, 2401-2406 (1992).

13. S. T. Balke, R. Thitiratsakul, R. Lew, P. Cheung, T. H. Morey, "A Strategy for Interpreting Multidetector Size-Exclusion Chromatography Data II: Application in Plastic Waste Recovery," in **Chromatography of Polymers**, T. Provder, ed., ACS Symposium Series, Washington, DC, 1993, pp. 199-219.

14. W. W. Yau, D. R. Hill, "Application of Triple-Detector GPC (RI-Visc-LS) for the Characterization of Brominated Polystyrene," in **Proceedings, International GPC Symposium**, Fl, 1994, pp. 25-46.

15. J. Lesec, M. Millequant, "Analysis of Star-Branched Polymers with Triple Detection GPC (RI, Viscometry, Light Scattering)," in **Proceedings, International GPC Symposium**, Fl, 1994, pp. 47-70.

16. R. Mendichi, A. Bolognesi, Z. Geng, A. G. Schieroni, "Molecular Characterization of Conducting Polymers, Poly(3-alkylthiophene), by Size Exclusion Chromatography with Single-Capillary Viscometer and Multi-Angle Light Scattering Detectors," in **Proceedings, International GPC Symposium,** Fl, 1994, pp. 827-838.

17. C. Jackson, H. G. Barth, D. E. Kirly, L. Chen, "Molecular Characterization of Hydroxylated Polyamides Using Size Exclusion Chromatography with Molecular-Weight-Sensitive Detectors," in **Proceedings, International GPC Symposium,** Fl, 1994, pp. 839-843.

18. J. Lesec, M. Millequant, M. Patin, P. Teyssie, " Star-Branched Polymers in Multidetection Gel Permeation Chromatography," in **Chromatographic Characterization of Polymers. Hyphenated and Multidimensional Techniques**, T. Provder, H. G. Barth, M. W. Urban, eds., ACS, Washington, DC, 1995, pp.167-179.

19. K. Sommermeyer, F. Cech, E. Pfitzer, Chromatographia, **25**, 167-168 (1988).

20. B. Tinland, J. Mazet, M. Rinaudo, Makromol. Chem., Rapid Commun., **9**, 69-71 (1988).

21. D. L.Williams, H. A. Pretus, R. B. McNamee, E. Jones, "Characterization of Medically Important Carbohydrate Polymers by Aqueous GPC with On-Line Multi-Angle Laser Light Scattering Photometry and Differential Viscometry Detectors," in **Proceedings, International GPC Symposium,** San Francisco, CA, 1991, pp. 181-193.

22. D. L. Williams, H. A. Pretus, I. W. Browder, J. Liq. Chromatogr., **15**, 2297-2309 (1992).

23. W. S. Bahary, M. P. Hogan, "Determination of Branching in Biopolymers by Size Exclusion Chromatography with Light Scattering (MALLS), Viscosity, and Refractive Index Detection," in **Proceedings, International GPC Symposium**, Fl, 1994, pp. 215-239.

24. A. M. Striegel, J. D. Timpa, "Comparison of Solution Behavior of Polysaccharides," in **Proceedings, International GPC Symposium**, Fl, 1994, pp. 567-591.

25. W. S. Bahary, M. P. Hogan, M. Jilani, M. P. Aronson, in **Chromatographic Characterization of Polymers. Hyphenated and Multidimensional Techniques**, T. Provder, H. G. Barth, M. W. Urban, eds., ACS, Washington, DC, 1995, pp.151-166.

26. C. Jackson, H. G. Barth, W. W. Yau, "Polymer Characterization by SEC with Simultaneous Viscometry and Laser Light Scattering Measurements," in **Proceedings, International GPC Symposium,** San Francisco, CA, 1991, pp. 751-764.

27. P. J. Wyatt, D. L. Hicks, C. Jackson, G. K. Wyatt, Amer. Lab., **20**, 108-113 (1988).

28. M. Bohdanecky, J. Kovar, **Viscosity of Polymer Solutions**, Elsevier, Amsterdam, 1982.

29. J. W. Mays, N. Hadjichristidis, "Polymer Characterization Using Dilute Solution Viscometry," in **Modern Methods of Polymer Characterization**, H. G. Barth, J. W. Mays, eds., John Wiley & Sons, Inc., New York, 1991, pp. 227-269.

30. E. W. Merrill, C. P. Dubbs, "Macromolecules as Coils, Rods, Stars, or Balls. Relationship between GPC, Intrinsic Viscosity, and Light Scattering" in **Proceedings, International GPC Symposium,** San Francisco, CA, 1991, pp. 1-21.

31. W. W. Yau, J. J. Kirkland, D. D. Bly, **Modern Size Exclusion Chromatography**, Wiley-Interscience, New York, 1979.

32. T. H. Mourey, S. M. Miller, S. T. Balke, J. Liq. Chromatogr., **13**, 435-452 (1990).

33. P. J. Wyatt, LC-GC, **15**, 160-168 (1997).

34. G. Eder, H. Janeschitz-Kriegl, S. Liedauer, A. Schausberger, W. Stadlbauer, G. Schindlauer, J. Rheol., **33**, 805-820 (1989).

35. J. P. Montfort, G. Marin, Ph. Monge, Macromolecules, **19**, 1979-1988 (1988).

36. J. P. Montfort, G. Marin, Ph. Monge, Macromolecules, **17**, 1551-1562 (1984).

37. B. H. Bersted, J. Appl. Polym. Sci., **30**, 3751-3765 (1985).

38. M. Potschka, Macromol. Symp., **110**, 121-154 (1996).

39. G. Glockner, **Gradient HPLC of Copolymers and Chromatographic Cross-Fractionation,** Springer Verlag, Berlin-Heidelberg-New York, 1991.

40. P. L. Dubin, J. I. Kaplan, B.-S. Tian, M. Mehta, J. Chromatogr., **515**, 37-42 (1990).

41. I. Gitsov, J. M. J. Frechet, Macromolecules, **27**, 7309-7315 (1994).

42. P. J. Flory, **Principles of Polymer Chemistry**, Cornell University Press, Ithaca, New York, 1953, Chapter 14.

43. K. F. Freed, **Renormalization Group Theory of Macromolecules**, John Wiley & Sons, New York, 1987, Chapter 10.

44. H. Yamakawa, **Modern Theory of Polymer Solutions**, Harper & Row, New York, 1971.

45. B. H. Zimm, Macromolecules, **13**, 592-601 (1980).

46. Y. Oono, M. Kohmoto, J. Chem. Phys., **78**, 520-528 (1983).

47. J. F. Douglas, K. F. Freed, Macromolecules, **17**, 2344-2354 (1984).

48. Y. Miyaki, Y. Einaga, H. Fujita, M. Fukuda, Macromolecules, **13**, 588-592 (1980).

49. T. H. Mourey, S. T. Balke, "A Strategy for Interpreting Multidetector Size-Exclusion Chromatography Data I," in **Chromatography of Polymers: Characterization by SEC and FFF**, ACS Symposium Series, T. Provder, ed., Washington, DC, 1993, pp. 180-198.

50. M. B. Huglin, J. Appl. Polym. Sci., **9**, 4003-4024 (1965).

51. C. M.Guttman, E. A. Di Marzio, J. F. Douglas, Macromolecules, **29**, 5723-5733 (1996).

52. P. L. Dubin, J. M. Principi, J. Chromatogr., **479**, 159-164 (1989).

53. A. E. Hamielec, H. J. Ederer, K. H. Ebert, J. Liq. Chromatogr., **4**, 1697-1707 (1981).

54. E. Grushka, Anal. Chem., **44**, 1733-1738 (1972).

55. C. Jackson, W. W. Yau, J. Chromatogr., **645**, 209-217 (1993).

56. W. W. Yau, S. W. Rementer, "A Computer Algorithm for Simultaneous SEC Retention and Column Dispersion Calibration," in **Proceedings, International GPC Symposium**, Ithaca, New York, 1987, pp. 148-167.

57. W. W. Yau, H. J. Stoklosa, D. D. Bly, J. Appl. Polymer Sci., **21**, 1911-1920 (1977).

58. A. E. Hamielec, J. Liq. Chromatogr., **3**, 381-392 (1980).

59. J. Billiani, G. Rois, K. Lederer, Chromatographia, **26**, 372-376 (1988).

60. A. E. Hamielec, A. C. Ouano, J. Liq. Chromatogr., **1**, 111-120 (1978).

61. D. Lecacheux, J. Lesec, C. Quivoron, J. Liq. Chromatogr., **5**, 217-228 (1982).

62. G. R. Meira, "Data Reduction in Size Exclusion Chromatography of Polymers," in **Modern Methods of Polymer Characterization**, H. G. Barth, J. W. Mays, eds., John Wiley & Sons, Inc., New York, 1991, pp. 67-101.

Received September 16, 1997
Accepted November 20, 1997
Manuscript 4615